J. Fluid Mech. (1980), *vol.* 101, *part* 1, *pp.* 33–51
Printed in Great Britain

The spreading of thin liquid films on a water–air interface

By M. FODA† AND R. G. COX
Department of Civil Engineering and Applied Mechanics, McGill University, Montreal, Quebec, Canada

(Received 21 August 1979 and in revised form 26 February 1980)

The spreading on a water–air interface of a thin liquid film is examined for the situation in which surface tension gradients drive the motion. A similarity solution is obtained numerically for unidirectional spreading when some general restrictions concerning the form of the liquid film constitutive relation is made. This solution gives the size of the film as a function of time and also the velocity and thickness distribution along the spreading film. Experiments are performed which show good agreement with the theory.

1. Introduction

The understanding of the phenomenon of the spreading of liquid layers on the surface of an immiscible supporting liquid has growing importance in ecology, environmental engineering and in the chemical and petro-chemical industry. For example, it is important to know how the size of an oil slick, resulting from oil spillage on the sea (e.g. from a leaking offshore oil well or from the wreck of an oil tanker), grows with time.

As a first step in the understanding of the hydrodynamics of spreading oil layers, Fay (1969) identified three basic mechanisms of spreading, and then, by simple dimensional reasoning, showed that early in the spreading of a large volume of liquid, gravitational forces cause the spreading which is resisted by the inertia forces arising from the slick's acceleration. As time elapses, viscous drag due to the substrate replaces inertia as the retarding force. Then after very long time, when the oil layer is very thin, possibly molecularly thin, surface tension replaces gravity as the driving agent. This latter spreading mechanism was further investigated by Di Pietro, Huh & Cox (1978) who derived the governing equations for such spreading films (which following Di Pietro *et al.* will be referred to as 'monolayers' whether they are of one or many molecules in thickness). Further spreading mechanisms may exist (Di Pietro *et al.* 1978; Di Pietro & Cox 1979, 1980) in limited regions or under special situations (such as when the oil is very viscous).

Di Pietro *et al.* (1978) argued that when oil (phase 1) spreads on the interface between water (phase 2) and air (phase 3), a band of oil of submicron thickness (i.e. a monolayer) would form ahead of the bulk of the oil‡ as a result of the imbalance of

† Present address: Department of Civil Engineering, MIT., Cambridge, Mass., U.S.A.

‡ The bulk of the oil is defined as that portion of the slick which is sufficiently thick so that (i) the oil may be considered as a continuum and (ii) the oil–water and oil–air interfaces have well defined constant interfacial tensions.

0022-1120/08/4565-2270 $02.00

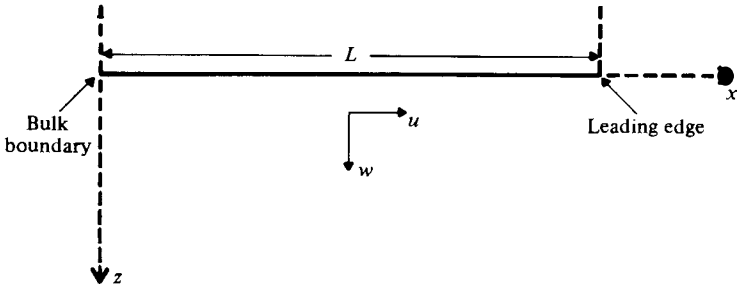

FIGURE 1. Spreading of monolayer on the surface of calm water with bulk boundary fixed at $x = 0$.

the interfacial tension forces at the contact line of the three phases (oil, water and air) which exists when the net spreading coefficient S_1 defined as (Harkins 1952),

$$S_1 \equiv \sigma_{23} - (\sigma_{12} + \sigma_{13}) \tag{1.1}$$

is positive; σ_{ij} is the interfacial tension between phases i and j.

The net force difference S_1 is assumed to be distributed along the monolayer so that the surface tension σ of the monolayer covered water surface varies from σ_{23} at the leading edge of the monolayer to the sum $(\sigma_{12} + \sigma_{13})$ at the boundary between the monolayer and the bulk of the oil (this boundary will be referred to as the bulk boundary). Assuming that there are no hysteresis or time dependent effects (i.e. there is, for example, no evaporation or dissolution of the oil in the water), the value of σ is related to the surface concentration h (volume per unit area) of the oil by the monolayer equation of state (Adamson 1967) so that

$$\sigma = \sigma(h). \tag{1.2}$$

Since h is zero at the leading edge and becomes very large (compared with its typical value) at the bulk boundary, the function $\sigma(h)$ must satisfy

$$\sigma(0) = \sigma_{23}, \quad \lim_{h \to \infty} \sigma = \sigma_{12} + \sigma_{13}.$$

In the present paper, we consider a monolayer spreading on a quiescent water surface in a unidirectional manner as would occur on water contained in a long channel. The bulk boundary is assumed to be held fixed at a certain position as the monolayer spreads. In §§ 2–6 a similarity solution to this problem is found while in §§ 7–9 an experiment is described which duplicates this situation. Good agreement is obtained between the theory and experiment.

2. Similarity solution

A monolayer is assumed to be spreading in the positive-x direction (figure 1) on water initially at rest with the bulk boundary stationary at $x = 0$ so that the monolayer length L in the x direction is a function of time t. We take the z-axis to be vertically downwards with $z = 0$ at the water surface, and assume no variation in monolayer thickness in the y direction. The oil-layer thickness h is then both a function of position x and time t. Furthermore oil must be continually supplied to the monolayer at $x = 0$

since the size and hence the volume of oil contained in the monolayer is expected to increase continuously with time.

If the monolayer constitutive relation (1.2) is satisfied by this spreading monolayer, it may be put in dimensionless form by letting

$$\sigma^* = \frac{\sigma - (\sigma_{12} + \sigma_{13})}{S_1}, \quad h^* = h/H, \tag{2.1}$$

where H is a characteristic value of h. Thus

$$\sigma^* = \sigma^*(h^*) \tag{2.2}$$

where $0 \leqslant \sigma^* \leqslant 1$ with $\sigma^*(0) = 1$ and $\sigma^*(h^*) \to 0$ as $h^* \to \infty$.

This dimensionless constitutive relation (2.2) for the oil film is assumed to be given in the following analysis.

If we let u, w be the velocity components in the x, z directions respectively, the governing equations for the induced flow in the water, the time-dependent boundary-layer equations, may be written as

$$\frac{\partial u}{\partial t} + u\frac{\partial u}{\partial x} + w^*\frac{\partial u}{\partial z^*} = \frac{\partial^2 u}{\partial z^{*2}}, \tag{2.3}$$

$$\frac{\partial u}{\partial x} + \frac{\partial w^*}{\partial z^*} = 0, \tag{2.4}$$

where the variables w^* and z^* are 'scaled' variables which are related to w and z by

$$z^* = z/\nu_2^{\frac{1}{2}}, \quad w^* = w/\nu_2^{\frac{1}{2}},$$

where ν_2 is the kinematic viscosity of the water.

Conservation of mass for the oil monolayer requires,

$$\frac{\partial h^*}{\partial t} + \frac{\partial}{\partial x}(u_0 h^*) = 0 \tag{2.5}$$

where $u_0(x, t)$ is the oil velocity (assumed constant across the oil layer in the z direction). The horizontal balance of forces in the monolayer gives (Di Pietro *et al.* 1978)

$$S_1\frac{\partial \sigma^*}{\partial x} + \tau_0 = 0 \tag{2.6}$$

where τ_0 is the shear stress exerted by the water on the oil in the x direction.

At the leading edge $x = L$ and at the bulk boundary $x = 0$ the conditions

$$h^* = 0, \quad \sigma^* = 1 \quad \text{at} \quad x = L \quad \text{and} \quad h^* \to \infty, \quad \sigma^* \to 0 \quad \text{as} \quad x \to 0 \tag{2.7a}$$

must be satisfied, while the kinematic boundary condition at the monolayer (which reduces to a condition of zero normal velocity since the interface is essentially horizontal) and the condition of no flow below the boundary layer ($z \to \infty$) yields

$$w^* = 0 \quad \text{on} \quad z^* = 0; \quad u \to 0 \quad \text{as} \quad z^* \to \infty. \tag{2.7b}$$

In addition since the velocity and stress in the water at the monolayer $z = 0$ are u_0 and τ_0 respectively,

$$u = u_0, \quad \frac{\partial u}{\partial z^*} = \frac{\nu_2^{\frac{1}{2}}}{\mu_2}\tau_0 \quad \text{on} \quad z^* = 0, \tag{2.7c}$$

where μ_2 is water viscosity. It should be noted that the characteristic layer thickness H does not appear in the above equations and boundary conditions. This implies that the velocity field and monolayer length do not depend on one's choice of H and only upon the dimensionless constitutive relation $\sigma^* = \sigma^*(h^*)$. Thus the value of H is arbitrary and can be chosen in any suitable manner. The last boundary condition in (2.7*c*) may be written as

$$\frac{\partial u}{\partial z^*} = \frac{\nu_2^{\frac{1}{2}} S_1}{\mu_2} \frac{d\sigma^*}{dx} \quad \text{on} \quad z^* = 0.$$

Hence, the solution depends only on the parameter $\beta \equiv \nu_2^{\frac{1}{2}} S_1/\mu_2$ so that, using dimensional analysis, we obtain for the monolayer length

$$L \propto \beta^{\frac{1}{2}} t^{\frac{1}{2}} \tag{2.8}$$

and for the velocity field in the water,

$$\bar{u} = f_1(\bar{x}, \bar{z}), \quad \bar{w} = f_2(\bar{x}, \bar{z})$$

where

$$\bar{u} = \beta^{-\frac{1}{2}} t^{\frac{1}{2}} u, \quad \bar{w} = \nu_2^{-\frac{1}{2}} t^{\frac{1}{2}} w, \tag{2.9a}$$

$$\bar{x} = \beta^{-\frac{1}{2}} t^{-\frac{1}{2}} x, \quad \bar{z} = \nu_2^{-\frac{1}{2}} t^{-\frac{1}{2}} z. \tag{2.9b}$$

In terms of these similarity variables the equations (2.3) and (2.4) for the motion in the boundary layer may be written as

$$-\tfrac{1}{4}\bar{u} - \tfrac{3}{4}\bar{x}\frac{\partial \bar{u}}{\partial \bar{x}} - \tfrac{1}{2}\bar{z}\frac{\partial \bar{u}}{\partial \bar{z}} + \bar{u}\frac{\partial \bar{u}}{\partial \bar{x}} + \bar{w}\frac{\partial \bar{u}}{\partial \bar{z}} = \frac{\partial^2 \bar{u}}{\partial \bar{z}^2}, \tag{2.10a}$$

$$\frac{\partial \bar{u}}{\partial \bar{x}} + \frac{\partial \bar{w}}{\partial \bar{z}} = 0 \tag{2.10b}$$

so that the number of independent variables is reduced from three (x, z, t) to two $(\bar{x}, \bar{z})$. Furthermore, by introducing a dimensionless stream function $\bar{\chi}$, defined by

$$\bar{u} = \frac{\partial \bar{\chi}}{\partial \bar{z}}, \quad \bar{w} = -\frac{\partial \bar{\chi}}{\partial \bar{x}}, \tag{2.11}$$

so that the continuity equation (2.10*b*) is automatically satisfied, it is seen that (2.10*a*) may be written in the form

$$-\tfrac{1}{4}\bar{\chi}_{,\bar{z}} - \tfrac{3}{4}\bar{x}\bar{\chi}_{,\bar{x}\bar{z}} - \tfrac{1}{2}\bar{z}\bar{\chi}_{,\bar{z}\bar{z}} + \bar{\chi}_{,\bar{z}}\bar{\chi}_{,\bar{x}\bar{z}} - \bar{\chi}_{,\bar{x}}\bar{\chi}_{,\bar{z}\bar{z}} = \bar{\chi}_{,\bar{z}\bar{z}\bar{z}}. \tag{2.12}$$

In a similar manner the monolayer equations (2.5) and (2.6) become

$$-\tfrac{3}{4}\bar{x}h^*_{\bar{x}} + (\bar{\chi}_{,\bar{z}}h^*)_{,\bar{x}} = 0, \tag{2.13a}$$

$$\bar{\chi}_{,\bar{z}\bar{z}} = -\sigma^*_{,\bar{x}} \quad \text{on} \quad \bar{z} = 0, \tag{2.13b}$$

while the boundary conditions (2.7) become

$$\left.\begin{aligned} &\sigma^* = 1, \quad h^* = 0 \quad \text{at the leading edge where } \bar{x} = \bar{x}^* \text{ say,} \\ &\sigma^* \to 0, \quad h^* \to \infty \quad \text{as} \quad \bar{x} \to 0, \\ &\bar{\chi} = 0 \quad \text{on} \quad \bar{z} = 0, \quad \bar{\chi}_{,\bar{z}} \to 0 \quad \text{as} \quad \bar{z} \to \infty, \\ &\bar{\chi}_{,\bar{z}} = \bar{u}_0 \quad \text{and} \quad \bar{\chi}_{,\bar{z}\bar{z}} = \bar{\tau}_0 \quad \text{on} \quad \bar{z} = 0, \end{aligned}\right\} \tag{2.14}$$

where

$$\bar{u}_0 = \beta^{-\frac{1}{2}} t^{\frac{1}{2}} u_0 \tag{2.15a}$$

and

$$\bar{\tau}_0 = \nu_2^{\frac{1}{2}} \beta^{-\frac{1}{2}} t^{\frac{1}{2}} \tau_0 / \mu_2. \tag{2.15b}$$

With $\bar{x} = \bar{x}^*$ at the leading edge, the length L of the monolayer is found from (2.9b) to be

$$L = \bar{x}^* \left[\frac{S_1^2}{\mu_2 \rho_2}\right]^{\frac{1}{4}} t^{\frac{1}{2}}. \tag{2.16}$$

Thus the problem is reduced to solving (2.12) and (2.13a, b) together with the boundary conditions (2.14) ,with the constitutive relation (2.2) being given.

It is instructive to examine the vorticity equation for the flow (u, w). Since, due to the boundary-layer approximation, $\partial w/\partial x \ll \partial u/\partial z$ the vorticity $\omega \simeq \partial u/\partial z$, so that in terms of the similarity variables

$$\bar{\omega} = \partial \bar{u}/\partial \bar{z} \quad \text{where} \quad \bar{\omega} = \nu_2^{\frac{1}{2}} \beta^{-\frac{1}{2}} t^{\frac{1}{2}} \omega.$$

If (2.10a) is differentiated with respect to $\bar{z}$, the vorticity equation is obtained as

$$\frac{\partial^2 \bar{\omega}}{\partial \bar{z}^2} = \frac{\partial}{\partial \bar{x}} [(\bar{u} - \tfrac{3}{4}\bar{x})\, \bar{\omega}] + \frac{\partial}{\partial \bar{z}} [(\bar{w} - \tfrac{1}{2}\bar{z})\, \bar{\omega}] + \tfrac{1}{2}\bar{\omega}. \tag{2.17}$$

The first two terms on the right-hand side can be considered as representing the convection of $\bar{\omega}$ in a flow field $(\bar{u} - \frac{3}{4}\bar{x}, \bar{w} - \frac{1}{2}\bar{z})$ whilst the last term represents the destruction of $\bar{\omega}$. The left-hand side represents diffusion of $\bar{\omega}$. Thus it is seen that the direction of vorticity convection in the $\bar{x}$ direction depends on the sign of the quantity $(\bar{u} - \frac{3}{4}\bar{x})$. However, by (2.16), the monolayer velocity at the leading edge in similarity variables is

$$\bar{u}_0(\bar{x}^*) = \beta^{-\frac{1}{2}} t^{\frac{1}{2}} \frac{dL}{dt} = \tfrac{3}{4}\bar{x}^*. \tag{2.18}$$

Also, the monolayer continuity equation (2.13a) may be written as,

$$\frac{\partial}{\partial \bar{x}} [(\bar{u}_0 - \tfrac{3}{4}\bar{x})\, h^*] + \tfrac{3}{4} h^* = 0$$

which when integrated from $\bar{x}$ to $\bar{x}^*$ gives

$$(\bar{u}_0 - \tfrac{3}{4}\bar{x})\, h^* = \tfrac{3}{4} \int_{\bar{x}}^{\bar{x}^*} h^*\, d\bar{x}. \tag{2.19}$$

Since the right-hand side of (2.19) is strictly positive (being zero only for $\bar{x} = \bar{x}^*$),

$$(\bar{u}_0 - \tfrac{3}{4}\bar{x}) > 0 \quad \text{for} \quad 0 \leqslant \bar{x} < \bar{x}^*. \tag{2.20}$$

If it is assumed that $\bar{u}$, like its value $\bar{u}_0$ on $z = 0$, is positive for all $\bar{z}$ at $\bar{x} = 0$ (and this will be later shown to be true when certain assumptions concerning the form of $\sigma^*(h^*)$ are made), then

$$\bar{u} - \tfrac{3}{4}\bar{x} > 0 \quad \text{for all } \bar{z} \quad \text{at} \quad \bar{x} = 0. \tag{2.21}$$

If it is also assumed that $\bar{u}$ near the leading edge (where $\bar{x} = \bar{x}^* - \hat{x}$ with $\hat{x}$ small) is a monotonic function of $\bar{z}$ (which will later be shown to be true), then

$$\bar{u} - \tfrac{3}{4}\bar{x} \leqslant 0 \quad \text{for all } \bar{z} \quad \text{on} \quad \bar{x} = \bar{x}^*, \tag{2.22}$$

with $\bar{u} - \frac{3}{4}\bar{x}$ decreasing from zero at $\bar{z} = 0$ to $-\frac{3}{4}x^*$ as $\bar{z} \to \infty$. Also

$$\bar{w} - \tfrac{1}{2}\bar{z} < 0 \quad \text{as} \quad \bar{z} \to \infty \quad \text{for} \quad 0 \leqslant \bar{x} \leqslant \bar{x}^*. \tag{2.23}$$

Thus by (2.21), (2.22) and (2.23) it is seen that for the region $0 < \bar{x} \leqslant \bar{x}^*$, $\bar{z} > 0$ the direction of the convection of $\bar{\omega}$ on the boundaries (not including $z = 0$) is everywhere into the region. Thus boundary layers must start forming (i.e. have zero thickness) at both $\bar{x} = 0$ and $\bar{x} = \bar{x}^*$, all the 'vorticity' $\bar{\omega}$ produced at $\bar{z} = 0$ being destroyed within the region ($0 \leqslant \bar{x} \leqslant \bar{x}^*, \bar{z} > 0$).

The formation of these two boundary layers at both ends of the region, which is peculiar to this problem, means that one should not solve the boundary layer equations starting from either end ($\bar{x} = 0$ or $\bar{x} = \bar{x}^*$) and proceed to the other. Instead the solution to the whole region should be obtained simultaneously in a manner similar to that necessary for an elliptic equation. Before obtaining the numerical solution by this means, it is necessary to find the asymptotic forms of the boundary layer near $\bar{x} = 0$ and $\bar{x} = \bar{x}^*$ due to the expected singular nature of the solution at these points.

3. Spreading behaviour near the bulk boundary $\bar{x} = 0$

It follows from (2.19) that for $\bar{x} \to 0$

$$(\bar{u}_0 - \tfrac{3}{4}\bar{x})\, h^* \sim K$$

where K is a positive constant $= \frac{3}{4}\int_0^{\bar{x}^*} h^*\, d\bar{x}$.

We now assume that

$$\bar{u}_0/(\tfrac{3}{4}\bar{x}) \to \infty \quad \text{as} \quad \bar{x} \to 0 \tag{3.1}$$

so that near $\bar{x} = 0$,

$$\bar{u}_0 h^* \sim K \tag{3.2}$$

giving the flow rate into the monolayer from the bulk as

$$u_0 h = K\beta^{\frac{1}{3}} H t^{-\frac{1}{3}}. \tag{3.3}$$

Near $\bar{x} = 0$, we assume that $\bar{u} \propto \bar{x}^n$ where n must be less than unity to satisfy (2.20) and (3.1). Also for $\partial h^*/\partial \bar{x} \leqslant 0$ as $\bar{x} \to 0$, n must be larger than or equal to zero [from (3.2)] so that

$$0 \leqslant n < 1. \tag{3.4}$$

Comparing the order of magnitude of the different terms in (2.10a), we see that the first three terms corresponding to the local time derivative $\partial u/\partial t$ in (2.3) are of order of $\bar{x}^n$ while the convective terms are of order of $\bar{x}^{2n-1}$. Thus as $\bar{x} \to 0$, the convective

terms dominate so that the boundary-layer equations (2.3) may, in the vicinity of the bulk boundary, be approximated by

$$u\frac{\partial u}{\partial x}+w^*\frac{\partial u}{\partial z^*}=\frac{\partial^2 u}{\partial z^{*2}},$$

$$\frac{\partial u}{\partial x}+\frac{\partial w^*}{\partial z^*}=0,$$

with

$$u=A(t)x^n, \quad w=0 \quad \text{on} \quad z^*=0$$

and

$$u\to 0 \quad \text{as} \quad z^*\to\infty.$$

Since the solution depends only on the parameter $A(t)$, the use of dimensional analysis gives

$$u=Ax^n f(\nu_2^{-\frac{1}{2}}A^{\frac{1}{2}}x^{\frac{1}{2}(n-1)}z) \tag{3.5}$$

so that

$$|\tau_0|=\mu_2\left|\frac{\partial u}{\partial z}\right|_{z=0}\propto x^{\frac{1}{2}(3n-1)}. \tag{3.6}$$

Now if we assume that as $h\to\infty$, the constitutive relation of the oil monolayer can be written as (Sheludko 1966)

$$\sigma\sim(\sigma_{12}+\sigma_{13})+Bh^{-p} \tag{3.7}$$

where B and p are constants, then from (3.3) we have that $h\propto x^{-n}$ so that

$$|\tau_0|=\left|\frac{d\sigma}{dx}\right|\propto x^{np-1}. \tag{3.8}$$

Therefore, from (3.6) and (3.8) we obtain,

$$n=\frac{1}{2p-3} \tag{3.9}$$

so that for $0\leqslant n<1$, we must have,

$$2<p\leqslant\infty. \tag{3.10}$$

If (3.5) is expressed in terms of the similarity variables $\bar{u}$, $\bar{x}$, $\bar{z}$ and use is made of the fact that $\bar{u}$ is a function of $\bar{x}$ and $\bar{z}$ only, it is seen that $A(t)$ has to be of the form

$$A\propto\left(\frac{\mu_2}{\nu_2^{\frac{1}{2}}S_1}\right)^{-(p-2)/(2p-3)}t^{-p/2(2p-3)}$$

so that

$$\bar{u}=\bar{x}^{1/(2p-3)}f(\eta) \tag{3.11a}$$

and

$$\bar{w}=\bar{x}^{-(p-2)/(2p-3)}g(\eta) \quad \text{where} \quad \eta=\bar{x}^{-(p-2)/(2p-3)}\bar{z}. \tag{3.11b}$$

Hence the stream function $\bar{\chi}$ must be of the form

$$\bar{\chi}=\bar{x}^{(p-1)/(2p-3)}\hat{\chi}(\eta). \tag{3.11c}$$

Substituting this into the time-independent boundary-layer equations (i.e. the equation (2.12) without the first three terms), we obtain

$$(2p-3)\hat{\chi}'''-(\hat{\chi}')^2+(p-1)\hat{\chi}''\hat{\chi}=0, \tag{3.12a}$$

the boundary conditions then being

$$\left.\begin{aligned}&\hat{\chi}=0 \quad \text{on} \quad \eta=0,\\ &\hat{\chi}'\to 0 \quad \text{as} \quad \eta\to\infty,\\ &\hat{\chi}'=f(0) \quad \text{on} \quad \eta=0.\end{aligned}\right\} \tag{3.12b}$$

This has a unique solution for any given value of $f(0)$. Consider the differential equation

$$(2p-3)\lambda'''-(\lambda')^2+(p-1)\lambda''\lambda=0 \tag{3.13a}$$

for $\lambda(\eta)$ with the boundary conditions

$$\lambda=0, \quad \lambda'=1 \quad \text{on} \quad \eta=0,$$

$$\lambda'\to 0 \quad \text{as} \quad \eta\to\infty. \tag{3.13b}$$

It is seen that $\hat{\chi}(\eta)$ is then

$$\hat{\chi}(\eta)=(f(0))^{\frac{1}{2}}\lambda\{(f(0)^{\frac{1}{2}})\eta\}. \tag{3.14}$$

Integration between zero and $\bar{x}$ of the relation,

$$-\frac{d\sigma^*}{d\bar{x}}=\bar{\tau}_0=\left.\frac{\partial\bar{u}}{\partial\bar{z}}\right|_{\bar{z}=0}\sim\bar{x}^{(3-p)/(2p-3)}f'(0)$$

yields

$$\sigma^*\sim -f'(0)\left(\frac{2p-3}{p}\right)\bar{x}^{p/(2p-3)} \quad \text{as} \quad \bar{x}\to 0. \tag{3.15}$$

The relation (3.7) may be written as

$$\sigma^*=B^*(h^*)^{-p} \quad \text{as} \quad h^*\to\infty \tag{3.16}$$

where $B^*=BH^{-p}S_1^{-1}$. Thus

$$h^*\sim\left(-\frac{(2p-3)f'(0)}{pB^*}\right)^{-1/p}\bar{x}^{-1/(2p-3)} \quad \text{as} \quad \bar{x}\to 0. \tag{3.17}$$

Using (3.2), this gives

$$\bar{u}_0\sim\left\{\frac{3}{4}\int_0^{\bar{x}^*}h^*d\bar{x}\right\}\left[-\frac{(2p-3)f'(0)}{pB^*}\right]^{1/p}\bar{x}^{1/(2p-3)} \quad \text{as} \quad \bar{x}\to 0, \tag{3.18}$$

which when compared with (3.11a) yields

$$f(0)=\frac{3}{4}\int_0^{\bar{x}^*}h^*d\bar{x}\left[-\frac{(2p-3)f'(0)}{pB^*}\right]^{1/p}. \tag{3.19}$$

From (3.11a), (3.11c) and (2.11) we obtain,

$$f'(0)=\hat{\chi}''(0)$$

which, using (3.14) gives,

$$f'(0)=[f(0)]^{\frac{3}{2}}\lambda''(0).$$

This when substituted into (3.19) gives,

$$f(0) = \left[\frac{3}{4}\int_0^{\bar{x}^*} h^*\, d\bar{x}\right]^{2p/(2p-3)} \left\{\frac{-(2p-3)\,\lambda''(0)}{pB^*}\right\}^{2/(2p-3)} \tag{3.20}$$

From this we conclude that a unique solution in this region cannot be found independently of what happens throughout the rest of the monolayer. This is because the value of $f(0)$ depends on the value of

$$\int_0^{\bar{x}^*} h^*\, d\bar{x}$$

which can only be found if the oil-thickness distribution over the whole monolayer region is known.

We now examine the solution $\lambda(\eta)$ satisfying (3.13a) with the boundary conditions (3.13b). Since this solution must approach the main stream condition exponentially (Goldstein 1965), we try as a first guess to the solution

$$\lambda_0(\eta) \sim A + e^{-b\eta} F(\eta) \tag{3.21}$$

where A and b are constants ($b > 0$) with $F(\eta)$ bounded for $\eta \to \infty$. Substituting (3.21) into (3.13a) and neglecting terms containing $e^{-2b\eta}$, it is seen that λ_0 satisfies

$$(2p-3)\,\lambda_0''' + (p-1)\,A\lambda_0'' = 0,$$

which has a solution satisfying $\lambda_0(0) = 0, \lambda_0'(\infty) = 0$ which is of the form (3.21), namely

$$\lambda_0(\eta) = A(1 - e^{-qA\eta}) \quad \text{where} \quad q = \frac{p-1}{2p-3}.$$

To improve this solution, we substitute λ_0 for the neglected terms in (3.13a) to obtain an equation for λ_1, an improved value of λ, as

$$(2p-3)\,\lambda_1''' + (p-1)\,A\lambda_1'' = (\lambda_0')^2 - (p-1)\,(\lambda_0 - A)\,\lambda_0''$$

and find a solution λ_1 that satisfies the conditions $\lambda_1(0) = 0, \lambda_1'(\infty) = 0$. In fact, we can improve the degree of accuracy by repeatedly using the formula

$$(2p-3)\,\lambda_m''' + (p-1)\,A\lambda_m'' = (\lambda_{m-1}')^2 - (p-1)\,(\lambda_{m-1} - A)\,\lambda_{m-1}'', \quad m = 1, 2, \ldots \tag{3.22}$$

with the boundary conditions $\lambda_m(0) = 0, \lambda_m'(\infty) = 0$. The solution λ_m will then be of the form,

$$\lambda_m(\eta) = A(1 + B\,e^{-qA\eta} + C\,e^{-2qA\eta} + D\,e^{-3qA\eta} + \ldots) \tag{3.23}$$

the value of A then being determined by the requirement that $\lambda_m'(0) = 1$. By examining the coefficients of the exponential terms for all possible values of p (i.e. for $2 < p \leqslant \infty$), it appears that the solution (3.23) for λ is convergent as $m \to \infty$ for all $\eta \geqslant 0$. Thus for example, the case $p = 3$ (for which $n = \frac{1}{3}$) has the solution (3.23) which may be written as

$$\lambda(\eta) = A[1 - 1{\cdot}1354\,e^{-\frac{2}{3}A\eta} + 0{\cdot}1582\,e^{-\frac{4}{3}A\eta} - 0{\cdot}0234\,e^{-2A\eta}$$

$$+ 0{\cdot}0006\,e^{-\frac{8}{3}A\eta} + \ldots] \quad \text{with} \quad A = 1{\cdot}3006.$$

For the case $p = \infty$ (for which $n = 0$), (3.13a) becomes

$$2\lambda''' + \lambda\lambda'' = 0 \tag{3.24}$$

with

$$\lambda = 0, \quad \lambda' = 1 \quad \text{at} \quad \eta = 0 \quad \text{and} \quad \lambda' \to 0 \quad \text{as} \quad \eta \to \infty.$$

This represents the laminar boundary-layer flow on a flat plane solid surface moving with constant velocity in its own plane in the positive-x direction while the solid surface is being continuously produced at $x = 0$ so that this end $x = 0$ is fixed in space. Sakiadis (1961) solved this problem numerically and his solution is in good agreement with the obtained series solution (3.23) which for this case ($p = \infty$) may be written as

$$\lambda(\eta) = A[1 - 1{\cdot}3090\, e^{-\frac{1}{2}A\eta} + 0{\cdot}3906\, e^{-A\eta} - 0{\cdot}0868\, e^{-\frac{3}{2}A\eta} + 0{\cdot}0052\, e^{-2A\eta} + \ldots] \quad \text{with} \quad A = 1{\cdot}6144.$$

4. Behaviour in the neighbourhood of the leading edge $\bar{x} = \bar{x}^*$

To obtain the solution of the boundary-layer equations (2.10) near the leading edge of the monolayer, we locate the origin of co-ordinates at the leading edge (i.e. at $\bar{x} = \bar{x}^*, \bar{z} = 0$) and introduce a variable $\hat{x}$ such that

$$\bar{x} = \bar{x}^* - \hat{x}.$$

From (2.18), $\bar{u} \to \frac{3}{4}\bar{x}^*$ on $\bar{z} = 0$ as $\hat{x} \to 0$. Thus, letting the boundary-layer thickness be proportional to $\hat{x}^q$ as $\hat{x} \to 0$, we see from an order-of-magnitude estimate of the different terms in (2.10) that $q = \frac{1}{2}$ so that in the limit of $\hat{x} \to 0$, (2.12) reduces to

$$\tfrac{3}{4}\bar{x}^*\bar{\chi}_{,\bar{z}\hat{x}} - \bar{\chi}_{,\bar{z}}\bar{\chi}_{,\bar{z}\bar{z}} + \bar{\chi}_{,\hat{x}}\bar{\chi}_{,\bar{z}\bar{z}} = \bar{\chi}_{,\bar{z}\bar{z}\bar{z}}. \tag{4.1}$$

Since $q = \frac{1}{2}$, we define $\eta = \bar{z}\hat{x}^{-\frac{1}{2}}$ and try as a solution $\bar{\chi} = \hat{x}^s\hat{\chi}(\eta)$ where, since

$$\bar{u} = \bar{\chi}_{,\bar{z}} \propto \hat{x}^0$$

as $\hat{x} \to 0$, s must be taken as $\frac{1}{2}$. Equation (4.1) then becomes

$$\hat{\chi}''' - \tfrac{1}{2}\hat{\chi}\hat{\chi}'' + \tfrac{3}{8}\bar{x}^*\eta\hat{\chi}'' = 0 \tag{4.2a}$$

with the boundary conditions

$$\hat{\chi} = 0, \quad \hat{\chi}' = \tfrac{3}{4}\bar{x}^* \quad \text{on} \quad \eta = 0$$

$$\hat{\chi}' \to 0 \quad \text{as} \quad \eta \to \infty. \tag{4.2b}$$

If we write $\hat{\chi}(\eta) = \frac{3}{4}\bar{x}^*\eta + \tilde{\chi}(\eta)$, then the equations and boundary conditions for $\tilde{\chi}$ are obtained as

$$\tilde{\chi}''' - \tfrac{1}{2}\tilde{\chi}\tilde{\chi}'' = 0$$

where

$$\tilde{\chi} = \tilde{\chi}' = 0 \quad \text{on} \quad \eta = 0; \quad \tilde{\chi}' \sim -\tfrac{3}{4}\bar{x}^* \quad \text{as} \quad \eta \to \infty. \tag{4.3}$$

Hence, $\tilde{\chi}$ is given by

$$\tilde{\chi} = -(\tfrac{3}{4}\bar{x}^*)^{\frac{1}{2}} g((\tfrac{3}{4}\bar{x}^*)^{\frac{1}{2}}\eta)$$

where g is the dimensionless stream function for the boundary-layer flow over a flat

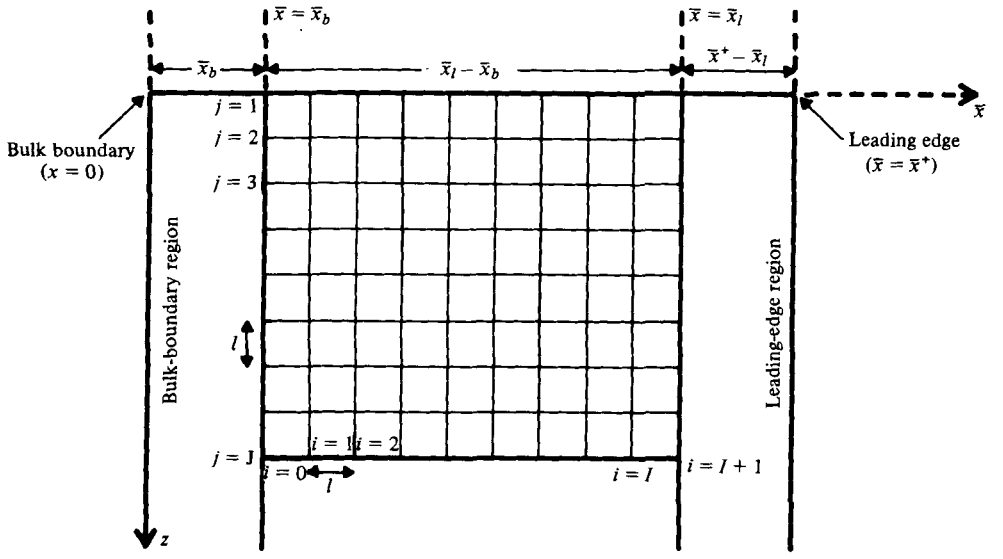

FIGURE 2. The finite difference square mesh connecting the leading edge region to the bulk boundary region.

plate (i.e. the Blasius boundary layer) (see Schlichting 1960). Thus the boundary layer near the leading edge is approximately the Blasius boundary layer with the monolayer there behaving like an advancing rigid flat plate. The solution for the function $g(\eta)$ is well known (see for example Howarth 1938). Thus

$$\bar{\chi} = \hat{x}^{\frac{1}{2}}[\tfrac{3}{4}\bar{x}^*\eta - (\tfrac{3}{4}\bar{x}^*)^{\frac{1}{2}} g((\tfrac{3}{4}\bar{x}^*)^{\frac{1}{2}}\eta)] \quad \text{as} \quad \hat{x} \to 0 \tag{4.4}$$

so that

$$\bar{\tau}_0 = -\frac{d\sigma^*}{d\bar{x}} = \frac{d\sigma^*}{d\hat{x}} = \bar{\chi}_{,\bar{z}\bar{z}}|_{\bar{z}=0} \sim \hat{x}^{\frac{1}{2}}[-(\tfrac{3}{4}\bar{x}^*)^{\frac{1}{2}} g''(0)] \quad \text{as} \quad \hat{x} \to 0.$$

Integrating this result between $\hat{x} = 0$ and a general value $\hat{x}$ and making use of the fact that $\sigma = \sigma_{23}$ [i.e. $\sigma^* = 1{\cdot}0$] at the leading edge ($\hat{x} = 0$), we obtain

$$\sigma^*(\hat{x}) \sim 1 - 2(\tfrac{3}{4}\bar{x}^*)^{\frac{1}{2}} g''(0)\, \hat{x}^{\frac{1}{2}} \quad \text{as} \quad \hat{x} \to 0. \tag{4.5}$$

From the monolayer equation of state [i.e. $\sigma^* = \sigma^*(h^*)$] one can then derive the asymptotic form of h^* for $\hat{x} \to 0$.

5. Solution procedure

Since the flow field changes rapidly near $\bar{x} = 0$ and $\bar{x} = \bar{x}^*$ (see §§ 3 and 4) we define near these two points a bulk boundary region ($0 \leqslant \bar{x} \leqslant \bar{x}_b$) and a leading edge region ($\bar{x}_l \leqslant \bar{x} \leqslant \bar{x}^*$) respectively where $\bar{x}_b$ and $\bar{x}^* - \bar{x}_l$ are small, and use in these regions the analytical solutions derived in §§ 3 and 4. For the remaining region ($\bar{x}_b \leqslant \bar{x} \leqslant \bar{x}_l$) a numerical computation is made using a finite difference method with a square grid (figure 2) with I and J nodal lines in the $\bar{x}$ and $\bar{z}$ directions respectively. The values of $\bar{\chi}, h^*, \bar{u}_0$ (and any partial derivatives of these quantities that are required) at the two edges $\bar{x} = \bar{x}_b$ and $\bar{x} = \bar{x}_l$ of the grid are then determined by the analytic solutions

in the bulk boundary and leading edge regions. Rather than considering $\bar{x}^*$ as an unknown it is more convenient to consider the grid size l as an unknown with the value of $\bar{x}^*$ then being determined by

$$\bar{x}^* = \bar{x}_b + l(I+1) + \hat{x}_l \tag{5.1}$$

where $\hat{x}_l = \bar{x}^* - \bar{x}_l$ is the length of the leading-edge region. Using the conventional Taylor series expansion method to approximate the various derivatives appearing in the governing equations (2.12), (2.13) and boundary conditions (2.14), the finite difference formulae are obtained (see for example Crandall 1956, p. 246). The finite difference equation that replaces (2.12) is applied at nodal points

$$(i,j)\,[1 \leqslant i \leqslant I \text{ and } 3 \leqslant j \leqslant J-2]$$

while the finite difference equation replacing the monolayer continuity equation (2.13a) is applied at mid-way between nodal points $i, i+1 [0 \leqslant i \leqslant I]$. The problem is thus reduced to solving a set of algebraic nonlinear equations for the values of $\bar{\chi}^{i,j}$ at the nodal points $(i,j)\,[1 \leqslant i \leqslant I, 2 \leqslant j \leqslant J]$, the values of $\bar{u}_0^i, h^{*i} [1 \leqslant i \leqslant I]$ and l (Foda & Cox 1977).

This set of nonlinear algebraic equations is replaced by an equivalent sequence of linear problems, the solution of which forms a sequence of solutions ($\bar{\chi}_n, \bar{u}_{0n}, h_n^*$ and l_n, $n = 0, 1, 2, \ldots$ where $n = 0$ corresponds to the initial assumed guess for the solution) which converges to the required solution as $n \to \infty$.

If the values of $\bar{\chi}_n^{i,j} (1 \leqslant i \leqslant I, 2 \leqslant j \leqslant J), (\bar{u}_0^i)_n\,(1 \leqslant i \leqslant I), h_n^{*i} (1 \leqslant i \leqslant I)$ and l_n are known, linear equations for $\bar{\chi}_{n+1}^{i,j}, (\bar{u}_0^i)_{n+1}, h_{n+2}^{*i}$ and l_{n+1} are found by writing formally

$$\begin{aligned} &\bar{\chi}_{n+1} = \bar{\chi}_n + \epsilon_1, \quad (\bar{u}_0)_{n+1} = (\bar{u}_0)_n + \epsilon_2, \\ &h_{n+1}^* = h_n^* + \epsilon_3, \quad l_{n+1} = l_n + \epsilon_4, \end{aligned} \tag{5.2}$$

where $\epsilon_i\,(i = 1, 4)$ are small quantities which tend to zero as $n \to \infty$. Then by substituting (5.2) into the nonlinear finite difference equations and neglecting quadratic terms in $\epsilon_i\,(i = 1, 4)$, we obtain equations which may be written in the matrix form

$$\mathbf{A}_n \mathbf{U}_{n+1} = \mathbf{C}_n \tag{5.3}$$

where $\mathbf{A}_n$ is an m by m dimensional matrix and $\mathbf{U}_{n+1}$ and $\mathbf{C}_n$ are m-dimensional vectors. $\mathbf{A}_n$ and $\mathbf{C}_n$ are functions of the known values of $\bar{\chi}_n^{i,j}, (\bar{u}_0^i)_n, h_n^*$ and l_n while $\mathbf{U}_{n+1}$ is the vector formed by the unknowns. The number of equations m is

$$m = IJ + I + 1$$

which is seen to be the same as the number of unknowns.

Examining the properties of matrix $\mathbf{A}_n$, we find that it is a square, non-symmetric, sparse matrix. Thus the conjugate gradient method (Hestenes & Stiefel 1952) is found to be the most suitable method of solution of (5.3) as far as convergence and stability are concerned. This method is essentially a relaxation method which was used because of its fast convergence for the solution of linear systems. Thus the solutions to the sequence of linear problems was found and continued until a solution was obtained that did not change with further iterations.

6. Numerical results

The computer program for the solution to this problem was designed to accept the monolayer constitutive relation (2.2) between σ^* and h^* in either analytical or tabulated form. In order to obtain, in a qualitative manner, the monolayer behaviour as it spreads on water the above numerical calculation was carried out for two analytical constitutive relations [$\sigma^* = \sigma^*(h^*)$] which were chosen to be

$$\sigma^* = \{\exp(-ah^*) + h^*\}^{-3} \tag{6.1}$$

with $a = \frac{2}{3}$ and $a = 1$. This form of $\sigma^*(h^*)$ was chosen so as to satisfy conditions:

(i) In the vicinity of the bulk boundary (as $h^* \to \infty$) $\sigma^* \sim h^{*-3}$ as suggested by Sheludko (1966);

(ii) In the vicinity of the leading edge (as $h^* \to 0$) $\sigma^* \sim 1 - Ah^{*\alpha}$ where A and α are constants.

In fact, for $h^* \to 0$, we have for $a \neq 1$,

$$\sigma^* \sim 1 - 3(1-a)h^* \quad \text{as} \quad h^* \to 0, \tag{6.2}$$

and for $a = 1$,

$$\sigma^* \sim 1 - 1{\cdot}5h^{*2} \quad \text{as} \quad h^* \to 0. \tag{6.3}$$

It should be noted that the linear relation (6.2) between σ^* and h^* as $h^* \to 0$ is of importance as this represents the case of a film in the gaseous phase (see Adamson 1967) this being a situation likely to occur for many liquid films when $h \to 0$. This situation occurs for one example ($a = \frac{2}{3}$) but not for the other.

The calculated velocity field $\bar{u}_0(\bar{x})$ along the monolayer and the oil layer thickness h^* are shown in figures 3 and 4 respectively for each of the assumed $\sigma^*(h^*)$ relations. It is seen that almost exactly the same results are obtained for the cases $a = \frac{2}{3}$ and $a = 1$. In fact the value of $\bar{x}^*$, determining the position of the leading edge (see (2.16)) was found to be equal to 1·39 for the example $a = \frac{2}{3}$ and equal to 1·36 for $a = 1{\cdot}0$. It is also noticed from figures 3 and 4 that although the asymptotic solution near the bulk boundary ($\bar{x} = 0$) was applied only close to the origin ($0 \leqslant \bar{x} \leqslant 0{\cdot}25$), the obtained solutions for $\bar{u}_0$ and h^* seem to obey approximately this asymptotic solution for much larger values of $\bar{x}$ (up to 0·6). Also, it is seen from the figures that the solutions for $\bar{u}_0$ and h^* do not deviate much from the leading edge asymptotic solution, (valid for $\bar{x}^* - 0{\cdot}1 \leqslant \bar{x} \leqslant \bar{x}^*$) when applied to much smaller values of $\bar{x}$ (down to $\bar{x} = 1{\cdot}1$ for which $\bar{x}^* - \bar{x} = 0{\cdot}3$). Computed velocity profiles $\bar{u}(\bar{z})$ in the boundary layer have been plotted in figure 5 for various values of $\bar{x}$ for the case $a = \frac{2}{3}$. It is observed that the boundary-layer thickness increases from zero at $\bar{x} = 0$ to a maximum at approximately $\bar{x} = 0{\cdot}85$ and thereafter decreases to zero at the leading edge ($\bar{x} = 1{\cdot}39$).

7. Experiment: Determination of $\sigma^*(h^*)$

The theory described in the previous sections was verified experimentally by examining the spreading of Dow Corning Silicone 200 fluid of 1000 cSt on the surface of distilled water at rest and contained in a Plexiglas rectangular channel ($120 \times 9 \times 5$ cm deep). This sat in a covered chamber to prevent atmospheric contamination (Foda & Cox 1977). The spreading fluid was deposited on the water surface by means of a

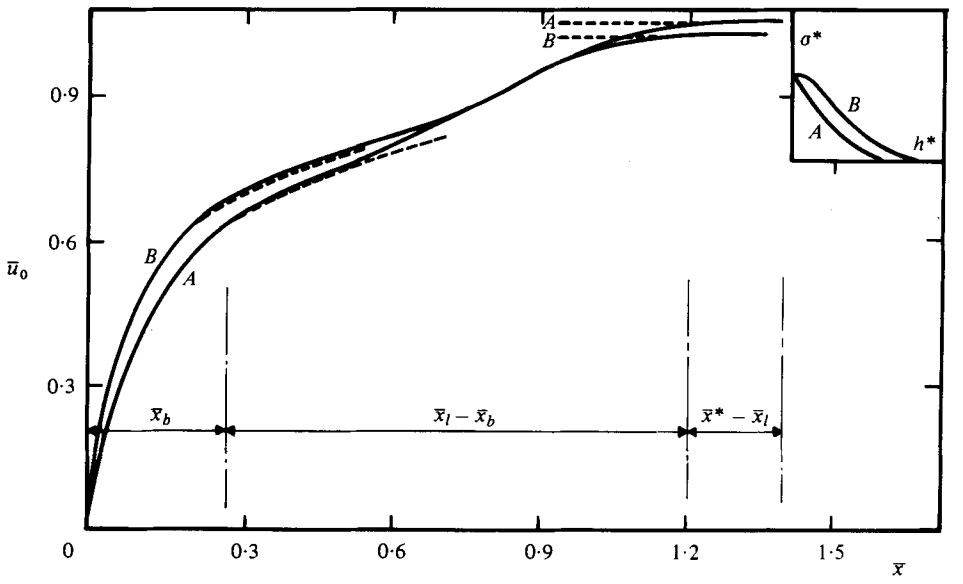

FIGURE 3. Dimensionless velocity field $\bar{u}_0$ along the spreading monolayer as a function of dimensionless position $\bar{x}$. Curves A and B refer to the results for the constitutive relation given by (6.1) with $a = \frac{2}{3}$ and $a = 1$ respectively. The dashed lines correspond to asymptotic solutions obtained for the bulk-boundary and leading-edge regions.

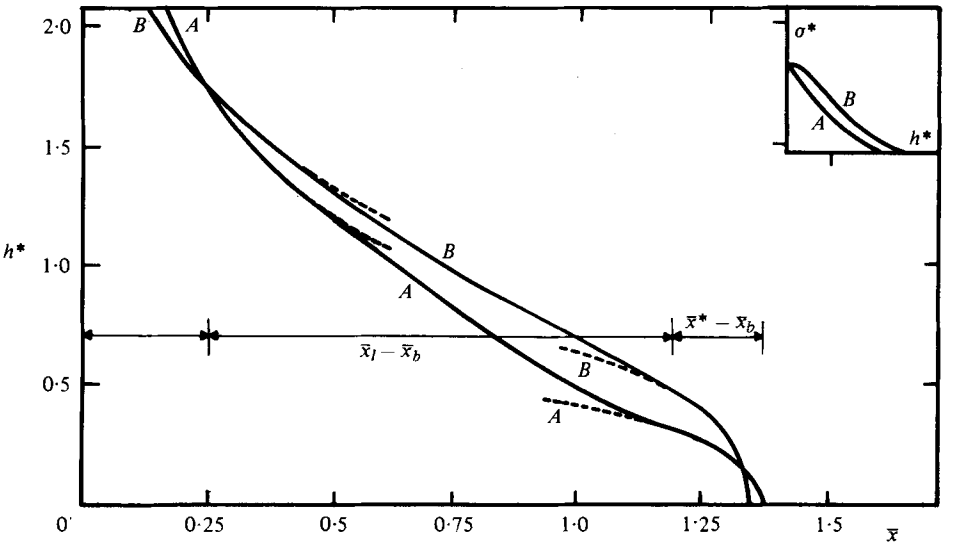

FIGURE 4. Dimensionless monolayer thickness h^* as a function of position $\bar{x}$. Curves A and B refer to results for the constitutive relation given by (6.1) with $a = \frac{2}{3}$ and $a = 1$ respectively. The dashed lines correspond to asymptotic solutions obtained for the bulk-boundary and leading-edge regions.

Plexiglas plate (9 × 3 cm) one longitudinal edge of which was trimmed to produce a sharp edge. This deposition was done by first spreading a thin uniform film of the Silicone fluid on the plate at and near the sharp edge. The plate was then placed across the width of the channel at one end and lowered so that the sharp edge just touched

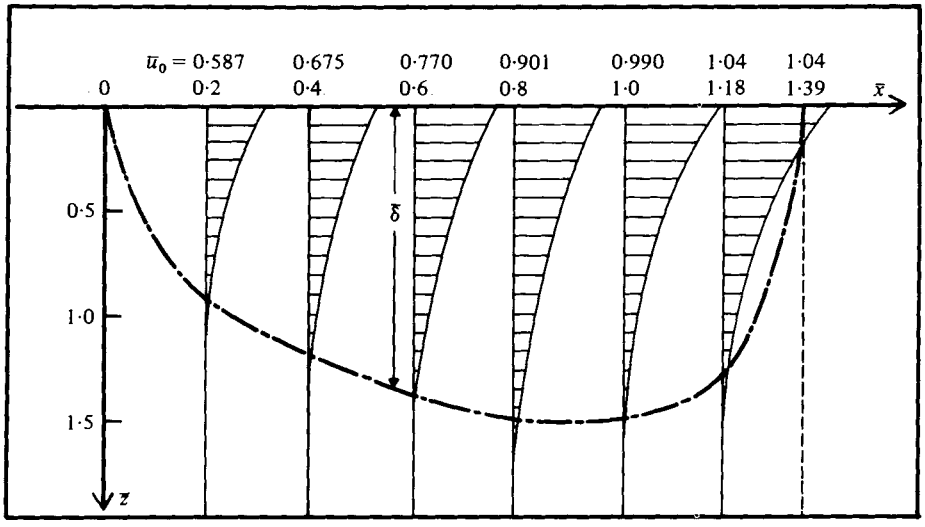

FIGURE 5. Boundary-layer velocity profiles $\bar{u}(\bar{z})$ for various positions $\bar{x}$ for the case with constitutive relation (6.1) with $a = \frac{2}{3}$. The dashed line shows how the boundary-layer thickness $\bar{\delta}$ (defined as the value of $\bar{z}$ at which $\bar{u}$ drops to $0{\cdot}05\ \bar{u}_0$) depends on position $\bar{x}$.

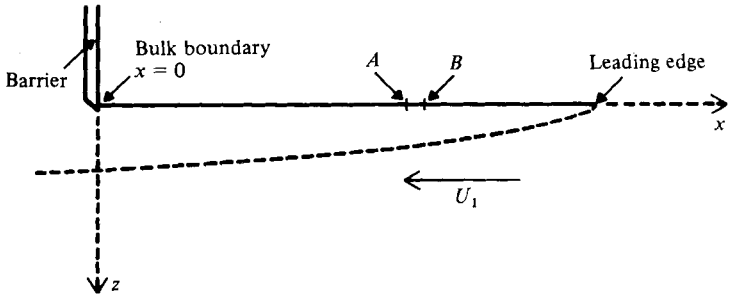

FIGURE 6. Spreading of monolayer against a uniform flow (of velocity U) with the bulk boundary fixed at $x = 0$.

the water surface. This ensured that there would be no gravity-viscous region (see Di Pietro *et al.* 1978) of spreading, the monolayer starting at the plate with a surface tension $(\sigma_{12} + \sigma_{13})$. Thus the conditions required for the theory are reproduced.

In order to compare the theory with experiment it is necessary to determine the constitutive relation $\sigma^* = \sigma^*(h^*)$ for the spreading liquid used. This was done by examining the steady state situation in which the Silicone fluid spreads against a uniform flow of the water along the channel mentioned above. This flow was produced by pumping the water along the channel. Thus after a uniform flow had been set up (with flow velocity of U_1 say), the Silicone fluid was deposited on the water surface at the downstream end using the Plexiglas plate as described above. The resulting monolayer then spread upstream against the flow and reached a steady state equilibrium position (as described by Di Pietro *et al.* 1978) as shown in figure 6. When this had occurred, the whole monolayer surface was then tagged by lightly sprinkling talcum powder on it (the talcum powder having been cleaned in the manner described by

Huh, Inoue & Mason 1975). The flow velocity along the channel was then reduced to a new value (U_2 say) so that the monolayer lengthened and formed a new steady state equilibrium. The resulting movement of the talcum-power particles was photographed using cinephotography. The distances between different pairs of neighbouring talcum-powder particles was measured for the two steady state equilibrium situations (corresponding to the flow velocities U_1 and U_2).

Thus if initially (with flow velocity U_1) the projected distance measured along the channel between neighbouring talcum powder particles A and B is AB (see figure 6) and if finally (with flow velocity U_2) the projected distance between the particles is $A'B'$, then by continuity

$$h_1^*(AB) = h_2^*(A'B') \tag{7.1}$$

where h_1^* and h_2^* are the values of h^* at the talcum-powder particles for the flow velocities U_1 and U_2 respectively. Also since the surface velocity $\mathbf{u}_0$ must be identically zero at all points on the monolayer for each of the steady state situations (see Di Pietro *et al.* 1978), the boundary layer in the water is of Blasius type so that for a flow velocity of U, the dimensionless surface tension σ^* of the monolayer covered water surface at a distance x from the point of deposition is obtained by integrating (2.6) with the known value of $\tau_0(x)$ for this boundary layer. Thus one obtains

$$S_1\{1-\sigma^*(x)\} = 0{\cdot}664[\mu_2\rho_2 U^3(L-x)]^{\frac{1}{2}} \tag{7.2}$$

where L is the monolayer length, which since $\sigma^* = 0$ at $x = 0$ (and $h^* = \infty$), must be given by

$$L = \frac{S_1^2}{(0{\cdot}664)^2\mu_2\rho_2 U^3} \tag{7.3}$$

so that (7.2) may be written as

$$\sigma^*(x) = 1-\{(L-x)/L\}^{\frac{1}{2}}. \tag{7.4}$$

Thus, using this result the value of σ^* can be calculated at the talcum-power particles for each of the steady state equilibrium positions. Thus the values σ_1^* and σ_2^* of σ corresponding to h_1^* and h_2^* may be found. By repeating this process for different neighbouring pairs of talcum-powder particles one can build up the relation between σ^* and h^*. Naturally the values of h^* obtained are arbitrary to the extent that they can all be multiplied by an arbitrary constant. However since this is equivalent to changing the definition of H, any convenient normalization of h^* (by choosing $h^* = 1$ at some point of the monolayer) may be adopted. In order to ensure that the relation (7.4) is valid, it was shown that for all experiments undertaken that (i) thickness of the boundary layers at the monolayer and channel bottom were much less than the water depth and (ii) the effect of the channel side walls were negligible.

The obtained relation between σ^* and h^* for the Silicone fluid used (1000 cSt) is plotted in figure 7 from which it is seen that σ^* decreases monotonically from 1 to 0 as h^* increases from zero. An examination of these results for values of $h^* > 4$ shows that the asymptotic form (3.7) for large values of h is satisfied with the index $p \simeq 2{\cdot}4$.

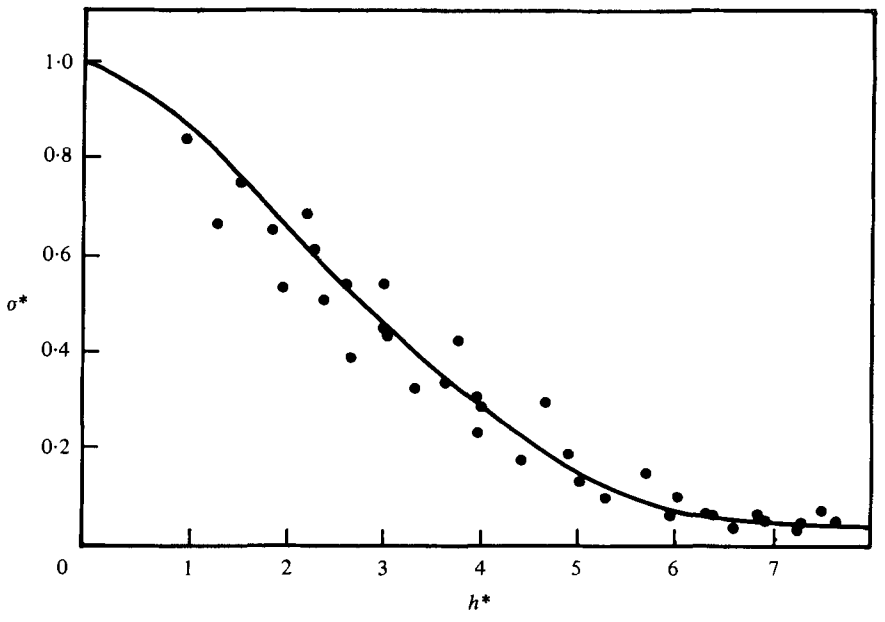

FIGURE 7. Experimentally determined constitutive relation $\sigma^* = \sigma^*(h^*)$ for the Dow Corning 200 Silicone (1000 cSt) monolayer.

8. Experiment: Time-dependent spreading of monolayer

To undertake the experiment corresponding to the situation (considered in §§ 2 to 6) where a monolayer spreads along a channel from a fixed position, the channel (described in § 7) was first filled with distilled water to a depth of 3·5 cm and left for 12 hours to allow the water to reach room temperature and to eliminate effects of water movement. The Silicone fluid (1000 cSt) was then deposited on the water surface at one end of the channel using the Plexiglas plate in the manner described in § 7. Both before and during the spreading of the monolayer along the channel, cleaned talcum-powder powder was sprinkled on the water surface just ahead of the point of deposition of the Silicone fluid. This was done by rotating a horizontal hollow cylinder with small holes in its surface which initially contained the talcum-powder powder. The movement of the talcum-powder particles on the moving monolayer was recorded by cine-photography and from an analysis of the film the velocity u_0 of the monolayer as a function of distance x (from the deposition point) and time t was derived.

9. Results and Discussion

From the monolayer velocity u_0 measured in the manner described in the previous section, $\bar{u}_0$ can be calculated as a function of $\bar{x}$ for various times t. This has been tabulated in table 1 from which it is observed that except for small values of $\bar{x}$ for which the experimental results were not accurate, the same value of $\bar{u}_0$ is obtained for all values of t if $\bar{x}$ is fixed. Thus $\bar{u}_0$ is a function only of $\bar{x}$ indicating that we have in fact reproduced experimentally a situation corresponding to the similarity solution considered in §§ 2 to 6. These experimental values of $\bar{u}_0$ have been plotted as a function of $\bar{x}$ in figure 8.

$\bar{x}$	Experimental values for $\bar{u}_0$ (calculated at various times t)								Average value of $\bar{u}_0 = \bar{u}_{av} = \frac{\Sigma \bar{u}_0}{n}$	Standard deviation in $\bar{u}_0 = \left(\frac{\Sigma(\bar{u}_0 - \bar{u}_{av})^2}{n}\right)^{\frac{1}{2}}$
0·1					0·697	0·586	0·581	0·380	0·553	0·114
0·2				0·700	0·701	0·683	0·685	0·500	0·653	0·08
0·3			0·689	0·710	0·729	0·69	0·70	0·682	0·70	0·016
0·4		0·722	0·700	0·735	0·730	0·730	0·715	0·728	0·720	0·011
0·5	0·781	0·781	0·76	0·75	0·77	0·77	0·77	0·77	0·77	0·0096
0·6	0·89	0·89	0·89	0·89	0·89	0·88			0·89	0·004
0·7	0·90	0·88	0·89	0·88	0·89				0·89	0·008
0·8	0 91	0 90	0·90	0·91					0·91	0·005
0·9	0·97	0·96	0·97						0·967	0·005
1·0 1·0	0·99								1·00	0·007
1·15 1·0	1·00								1·00	0·00

TABLE 1. Values of $\bar{u}_0$ as a function of $\bar{x}$ obtained from the experimentally obtained values of $u_0(x, t)$ along the monolayer.

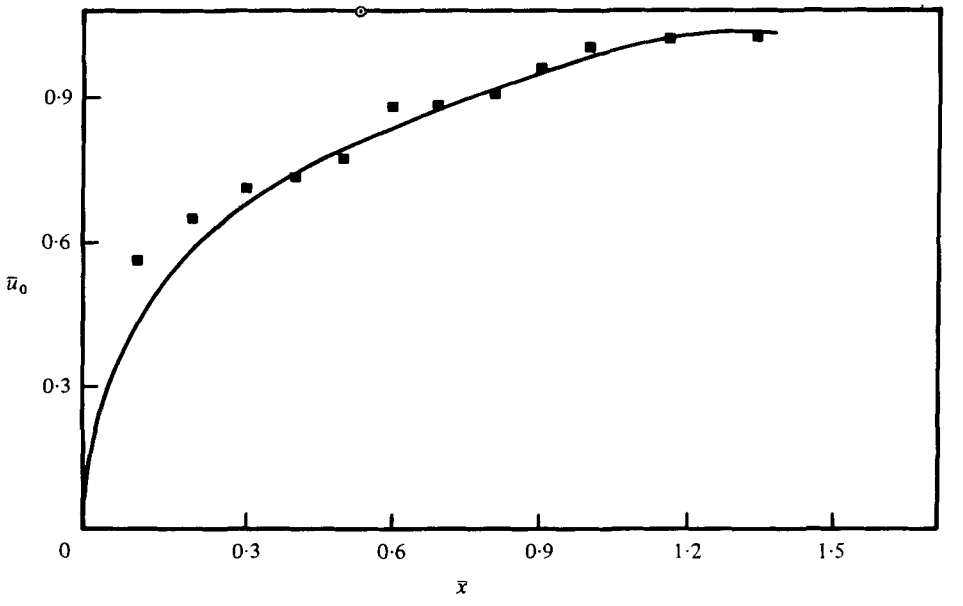

FIGURE 8. Comparison between the theoretical (solid line) velocity field $\bar{u}_0(\bar{x})$ along the monolayer and the experimental values ($\bar{u}_{av}$ in table 1) for the Dow Corning 200 Silicone (1000 cSt) monolayer.

For the constitutive relation $\sigma^* = \sigma^*(h^*)$ determined experimentally (see § 7) for the Silicone fluid (1000 cSt), the numerical computation discussed in § 6 was used to obtained theoretically the value of $\bar{u}_0$ as a function of $\bar{x}$ for the similarity solution. This has also been plotted on figure 8 from which it is seen that there is good agreement with the experimental results. In particular the value of $\bar{x}^*$ (which determines how the leading edge moves) is found to be 1·375 for the computed similarity solution and to be 1·33 from the experimental results.

It has been noted from figures 3 and 4 that the form of the constitutive relation $\sigma^* = \sigma^*(h^*)$ seems to have little influence on the similarity solution (at least for the examples considered here). In fact the two examples considered in § 6 give values of $\bar{x}^*$ equal to 1·36 and 1·39 while the relation $\sigma^* = \sigma^*(h^*)$ for the Silicone fluid (1000 cSt) gave $\bar{x}^* = 1{\cdot}375$.

It should also be noted that the experiments on monolayer spreading by Huh *et al.* (1975), Garrett & Barger (1970) and Lee (1971), although not designed to reproduce the similarity solution discussed here, also gave values of $\bar{x}^*$ of approximately 1·33.

This work was supported by the Natural Sciences and Engineering Research Council of Canada under Grant A7007.

REFERENCES

ADAMSON, A. W. 1967 *Physical Chemistry of Surfaces*, cha. 3. Wiley-Interscience.

CRANDALL, S. H. 1956 *Engineering Analysis, A Survey of Numerical Procedure*, p. 246. McGraw-Hill.

DI PIETRO, N. D. & COX, R. G. 1979 *Quart. J. Mech. Appl. Math.* **32**, 355.

DI PIETRO, N. D. & COX, R. G. 1980 *J. Fluid Mech.* **96**, 611.

DI PIETRO, N. D., HUH, C. & COX, R. G. 1978 *J. Fluid Mech.* **84**, 529.

FAY, J. A. 1969 The spread of oil slicks on a calm sea. In *Oil on the Sea* (ed. D. P. Hoult), pp. 53–63. Plenum.

FODA, M. A. & COX, R. G. 1977 *Dept. of Civil Engng, McGill Univ. Tech. Rep.* no. 77-1 (FML).

GARRETT, W. D. & BARGER, W. R. 1970 *Environ. Sci. Tech.* **4**, 123.

GOLDSTEIN, S. 1965 *J. Fluid Mech.* **21**, 33.

HARKINS, W. D. 1952 *The Physical Chemistry of Surface Films*. Reinhold.

HESTENES, M. R. & STIEFEL, E. 1952 *J. Res. Nat. Bureau of Standards*, no. 2379.

HOWARTH, L. 1938 *Proc. Roy. Soc.* A **164**, 547.

HUH, C., INOUE, M. & MASON, S. G. 1975 *Can. J. Chem. Engng* **53**, 367.

LEE, R. A. S. 1971 A study of the surface tension controlled regime of oil spread. M.S. thesis (Mech. Engng), Massachusetts Institute of Technology.

SAKIADIS, B. C. 1961 *A.I.Ch.E. J.* **7**, 221.

SCHLICHTING, H. 1960 *Boundary Layer Theory*. McGraw-Hill.

SHELUDKO, A. 1966 *Colloid Chemistry*, cha. 6. Elsevier.